Engineering Journal issn: 0125-8281

Article

Effect of the Sliding of Stacked Live Loads on the Seismic Response of Structures

Surya Prakash Challagulla[1,a], **Chandu Parimi**[1,b,*], **and P. K. Thiruvikraman**[2,c]

1 Department of Civil Engineering, BITS-Pilani, Hyderabad 500078, India
2 Department of Physics, BITS-Pilani, Hyderabad 500078, India
E-mail: [a]p20150407@hyderabad.bits-pilani.ac.in, [b]parimi@hyderabad.bits-pilani.ac.in (Corresponding author), [c]thiru@hyderabad.bits-pilani.ac.in

Abstract. Dynamic interaction between sliding live loads and the structure they act on is significant in the seismic analysis and design of the structure. The problem becomes more complex when the live loads are in the form of stacks. This paper presents a numerical model to simulate the dynamic interaction between a primary structure (PS) and a set of stacked bodies lying on it. Individual bodies in the stack were termed as secondary bodies (SBs) in this study. The lowest SB in the stack interacts with the structure through friction. Similar frictional forces also exist between different levels of the stack. This numerical model was verified with a Finite Element model. A parametric study was performed on the seismic response by varying the dynamic properties of the structure and SBs. The energy dissipation is found to be significant due to sliding within the stack. A novel methodology is proposed to calculate a modified structural period (T_{new}) of the structure to use in its design. It was found that the T_{new} varies significantly with the structural period, mass ratios, and coefficients of friction. Finally, design equations are proposed to calculate the T_{new}. Two Indian seismic hazard levels were considered for this study.

Keywords: Primary structure, secondary bodies, coulomb friction, stacked loads, sliding.

ENGINEERING JOURNAL Volume 24 Issue 4
Received 12 February 2020
Accepted 6 May 2020
Published 31 July 2020
Online at https://engj.org/
DOI:10.4186/ej.2020.24.4.97

DOI:10.4186/ej.2020.24.4.97

1. Introduction

Various loads need to be considered in the seismic design of any structure. Determination of the self-weight of a structure is easy, but the calculation of live loads is a difficult task [1]. Building design standards provide inadequate regulations on how to include them in the seismic structural analyses. Standards like ASCE/SEI 7-10 (2010) indicate that the portion of live load mass to be included as inertia is 25% in facilities used for storage. However, this percentage falls to 10% in guidelines that are applicable to marine structures [1]. Live loads that exceed 4.79 kN/m^2 shall not be reduced according to ASCE/SEI 7-10 (2010) and reduced by 50%, according to IS: 1893-2016. The suggested percentages are based on the assumption that only a minor portion of the live load is likely to be present during a seismic event [1]. Pile supported storage structures, and scaffolding structures with lead blankets are structures with nearly permanent live loads. Hence proper quantification of live loads is required since design becomes conservative if the whole live loads are considered as part of the dead loads. This is especially true for light structures (where live loads are considerable compared to dead loads). The PS design becomes unsafe if live loads are completely neglected.

The behavior of sliding rigid blocks under base excitations is a complex problem of dynamics that have been studied extensively for many decades. The response of a rigid block resting on a foundation with a periodic excitation has been studied [2] and is found not to slip when the frequency ratio exceeds one. The effect of base excitation frequency on a free-standing rigid block [3] has been studied, and it was found that base excitation frequency plays a vital role in determining the stability of rigid blocks. Sliding displacement of an unanchored body subjected to earthquake excitation is estimated [4]. Sliding and overturning analysis of a free-standing cask under earthquakes [5] has been studied. As per this study, the sliding distance of the body depends upon the earthquake intensity and coefficient of friction. Simulation of free-standing relics under earthquake loads showed that sliding response increases with an increase of earthquake strength [6]. Sliding and rocking motions of a free-standing structure coupled with the inner structure are studied [7]. These studies focused on the dynamic response of the sliding bodies under base excitations. Such studies are required to develop suitable anchorage mechanisms for equipment or containers that contain hazardous materials.

The dynamic behavior of a linear spring and a dashpot supporting a rigid body with the possibility to slide is investigated [8]. It was found that significant slippage occurs for smaller frequency ratios and resonance bands of frequencies. It was also deduced that slippage increased when the mass of structure was small relative to that of the block. The resonance response of a steel structure with sliding floor loads is also studied [9]. The results of their study concluded that the response of the oscillator with a sliding load system is influenced by mass ratio and frictional coefficient. The effect of live loads on the dynamic response of structures has been studied [10]. The authors compared the structure's drift when the live load has a flexible connection to the structure's drift when the live load object is rigidly attached. Finite element modeling of a single-degree (SDOF) structure with a rigid sliding block has been studied [11].

While the above research focuses on the dynamic behavior of sliding bodies, very little work has been done in understanding the dynamic behavior of structures supporting these rigid blocks. A design expression is proposed to estimate the portion of the live load to be included as inertia in the seismic design of the primary structure [12]. The authors reported that a portion of the live load to be included is a function of total structural acceleration and frictional coefficient at the live load object-structure interface. Design expression proposed by the authors [12] is verified against the experimental study [13] by means of a shake table test conducted on an SDOF supporting structure with a sliding block. The authors concluded that effective live load as inertia depends upon the level of excitation and dynamic properties of the structure. A study [14] on the multi-degree of freedom (MDF) framed shear buildings with the rigid sliding blocks has been studied. A parametric study was done to quantify the effective portion of a live load that contributes to the seismic weight.

The above studies are limited to the effect of single sliding live load objects on structures. However, stacks are sometimes part of live loads. These stacks can have sliding surfaces within their various layers. Such stacks are widely seen in docks and storage structures (pile-supported container terminals). By considering these container stacks as a single object by neglecting the energy dissipation due to friction between the layers, the response of the structure can be overestimated [12]. This is the main concern of the present study. The container stacks may undergo sliding, rocking, and combined sliding –rocking under external excitations. In the present study, squat container stack (one on the top of the other) of two rigid bodies which show only sliding mode of vibration when the acceleration demand of the structure-block system exceeds the limiting friction is considered. This paper presents a numerical model to simulate the dynamic interaction between different levels of the stack and also between the stack and the structure. In this study, a numerical model is developed by considering the nonlinearity due to the sliding of the blocks. The nonlinearity due to the yielding of the structure is not considered. Coupled nonlinearity due to sliding of the rigid blocks and the yielding of the primary structure will be considered, and the present study can be further extended in the future since the nonlinear study gives the more generalized response of the structure [15]–[19]. The numerical model developed is further incorporated in a methodology to determine the modified structural period of the PS (T_{new}) with a stack of objects under real earthquake excitations.

2. Problem Statement

The seismic behavior of a primary structure with a stack of sliding live load objects on it is investigated under real earthquake excitations. Ground motions compatible with the given seismic hazard spectrum are used in this analysis. The governing equations of motion of the primary and secondary masses are developed considering Coulomb's friction model and were solved using the fourth-order Runge-Kutta method. Following are the assumptions made in this study:

- Single-degree primary structure is considered, and it is linearly elastic.
- Static and Kinematic coefficients are equal to each other at each surface of the system
- Live load objects are sufficiently squat so they can slide but do not show any rocking failure.

3. Mathematical Formulation

The mathematical formulation involves the derivation of the dynamic equations of motion of the single-degree primary structure (PS) with the n number of secondary bodies (SBs) as a stack. To derive the equations of motion of the PS and sliding SBs, the following methodology is formulated:

1. Start from the top most mass in the stack, i.e., n^{th} body (m_n).
2. Check sliding condition (Eq. (1)) at every interface in the stack moving downwards.
3. While moving downwards, find the clusters sticking to each other.
4. Assume each cluster to be an individual body, and all such clusters are sliding w.r.t. each other.
5. Derive the dynamic equations of motion for the clusters (Eq. (2) and (3)) and solve them.

For the above steps 1 and 2, a sliding condition is to be defined. Note that as the calculation moves from the topmost body downwards, the sliding conditions provide the clusters. Let the q^{th} body be the topmost body of the cluster that the i^{th} body belongs to. Hence there would be $(q-i)$ bodies stuck to the i^{th} body above it.

A function $\boldsymbol{slip_i}$ is defined to check the sliding behaviour between the $i^{th}$and $(i-1)^{th}$ bodies.

$$\boldsymbol{slip_i} = \left[(\ddot{u}_{i-1} + \ddot{u}_g)\sum_{j=i}^{q} m_j + \mu_{k_{q+1}} g.sign(\dot{u}_{q+1} - \dot{u}_q)\sum_{j=q+1}^{n} m_j\right] \geq \mu_{s_i} g \sum_{j=i}^{n} m_j \quad (1)$$

If $\boldsymbol{slip_i}$ = 1 (True), then i^{th} body slides with respect to $(i-1)^{th}$ body.

= 0 (False), the i^{th} body sticks to the $(i-1)^{th}$ body

It should be noted that $\boldsymbol{slip_i}$ is also used to check the sliding between the bottom-most body of a stack (m_{b1}) and the primary structure (m_p).

Figure 1(a) shows the primary structure with a n number of SBs in the various levels of the stack. By using the condition for sliding $\boldsymbol{slip_i}$, relative motion between the different levels of the stack is verified, and corresponding clusters are defined as shown in Fig. 1(b). The dynamic equations of motion can be written as follows:

Assume PS is part of the 1^{st} cluster, and there are C clusters above it.

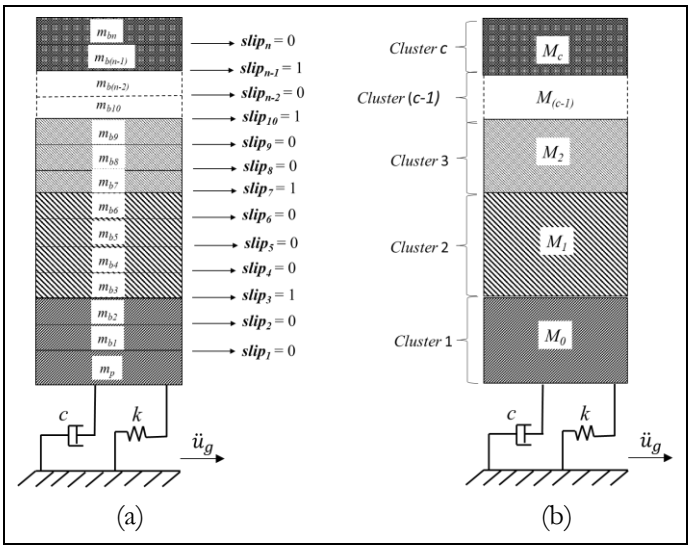

Fig. 1. Clusters formation.

$$M_0(\ddot{U}_p + \ddot{u}_g) + c\dot{U}_p + kU_p = \mu_{k_1}\left(\sum_{j=1}^{C} M_j g\right) g.sign(\dot{U}_2 - \dot{U}_p) \quad (2)$$

where M_0 is the mass of the 1^{st} cluster. μ_{k_1} is the kinematic coefficient of friction between the interfaces of the 1^{st} cluster and the above cluster. U_p, U_2, are the displacements of the 1^{st} and above clusters, respectively.

The dynamic equation of motion for the l^{th} cluster:

$$M_l(\ddot{U}_l + \ddot{u}_g) = -\mu_{k_l}\left(\sum_{j=l}^{C} M_j\right) g.sign(\dot{U}_l - \dot{U}_{l-1}) + \mu_{k_{l+1}}\left(\sum_{j=l+1}^{C} M_j\right) g.sign(\dot{U}_{l+1} - \dot{U}_l) \quad (3)$$

where M_l is the mass of the l^{th} cluster. μ_{k_l} is the kinematic coefficient of friction between the interfaces of the l^{th} cluster and the $(l-1)^{th}$ cluster, whereas $\mu_{k_{l+1}}$ is friction coefficient between the $(l+1)^{th}$ cluster and the l^{th} cluster, respectively. U_{l-1}, U_l, U_{l+1} are the displacements of the $(l+1)^{th}$, l^{th} and $(l-1)^{th}$ clusters respectively. The numerical analysis procedure is shown as the flow chart in Fig.2.

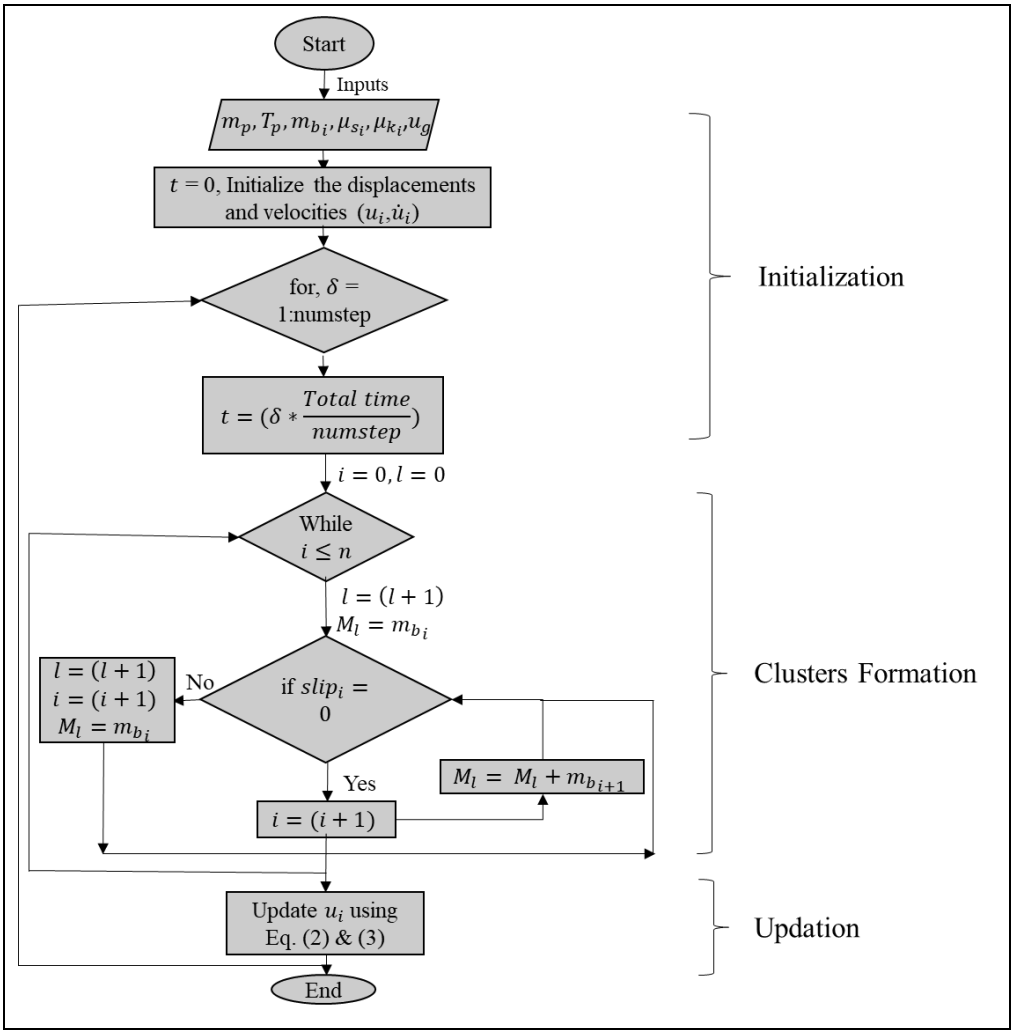

Fig. 2. The flowchart of the numerical anlaysis procedure.

The present study examines the effect of the two-level stack of SBs on the seismic behaviour of the structure. The idealization of a single-degree primary structure (PS) with a mass m_p, lateral stiffness k, and viscous damping c with such a stack on it is shown in Fig. 3. The mass of the secondary bodies is represented as m_{b1} and m_{b2}. The bottom secondary body (SB_1) in the stack is assumed to be connected to the structure by Coulomb friction, and such friction is also present between the bodies (SB_1 and SB_2) in the stack. The static (μ_s) and kinetic (μ_k) coefficients of friction are assumed to be equal and called as μ in this study. Let u_p, u_{b1} and u_{b2} are the displacements of PS and SBs, respectively with respect to ground. The combined system is subjected to a ground acceleration of $\ddot{u}_g$.

The governing dynamic equations of motion (Eqs. (2) and (3)) for the structure and the stack in stick and sliding/slip mode are solved by the 4th order Runge-Kutta method. In the subsequent discussion, mass ratios (α_i) of the stack of live load objects, the mass ratio (α) of single sliding live load object and original structural period (T_p) are introduced and defined as:

$$\alpha_i = \frac{m_{bi}}{m_p} \tag{4}$$

$$\alpha = \sum_{i=1}^{n} \alpha_i \tag{5}$$

$$T_p = 2\pi\sqrt{\frac{m_p}{k}} \tag{6}$$

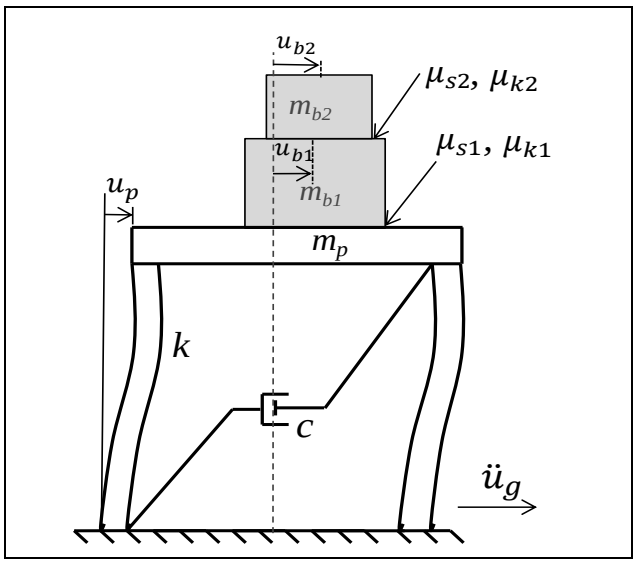

Fig. 3. Idealization of single-degree primary structure with two level stack of SBs.

4. Selection of Ground Motions

In order to capture the effect of the sliding bodies on the dynamic behaviour of the structure, 11 earthquake excitations are selected from the PEER NGA ground motion database [20], which is the minimum number of ground motions required for the analysis as per ASCE 7-16 [21] and applied to it. The moment magnitude (M_w) of the selected excitations varies from 6.2 to 7.36 to represent a wide range of magnitudes. Excitations are selected based upon the shear wave velocity (V_{S30}) of 360-760 m/s to represent hard soil conditions as per the National Earthquake Hazard Reduction Program (NEHRP) site classification system. Excitations are made compatible with the hard soil response spectra associated with Seismic zones III and V, which respectively represent zones of medium and highest damage risk zones given in the IS 1893:2016 [22]. Spectrum compatible ground motions are utilized in this study since they can reduce the computational effort significantly compared to multiple sets of ground motions [23]. The spectral matching method in the time domain proposed by [24] is utilized to generate the spectrum compatible earthquake excitations. The details of the excitations are shown in Table 1. Figure 4 shows the IS 1893:2016 spectra as a target spectra associated with 5% damping. Figure 5 shows the 5%-damping mean response spectra of the 11 earthquake excitations. The average spectrum or mean spectrum does not fall below 90% of the target spectrum in the entire period range as per the requirement in ASCE 7-16.

5. Validation of the numerical model

The numerical solution of the displacement response of a structure with the stack of sliding bodies is compared to the results from a Finite Element (FE) model for validation purposes. In this section, the main features of a FE model developed using ABAQUS/CAE release 6.14 (academic version) are described. The basic FE model developed consists of a rectangular body that simulates the primary structure with sliding rigid blocks resting on it. The rigid blocks and primary structure are modelled as discrete rigid bodies. The developed FE model is used to calculate the response of a single-degree oscillator with sliding rigid blocks resting on it. To do so, a horizontal spring element and dashpot were attached to the rectangular body to simulate the oscillator, as shown in Fig. 6.

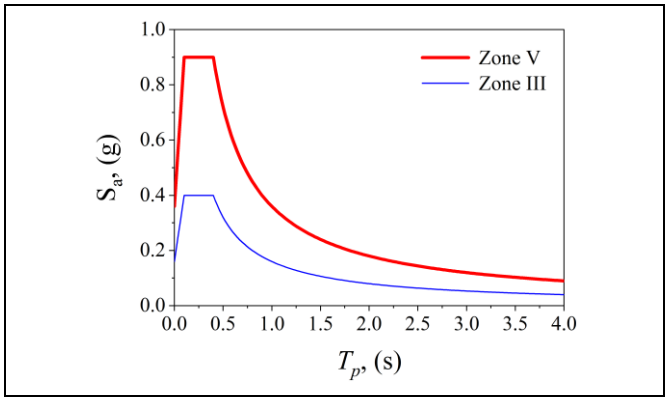

Fig. 4. IS 1893:2016 Zone III and Zone V design spectra for hard soil.

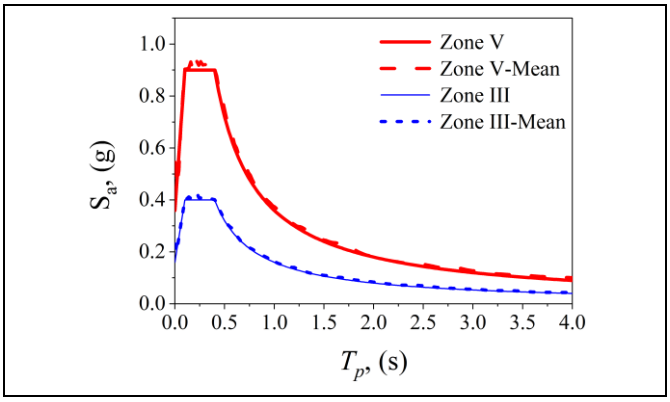

Fig. 5. Target and mean acceleration spectra for 5% damping.

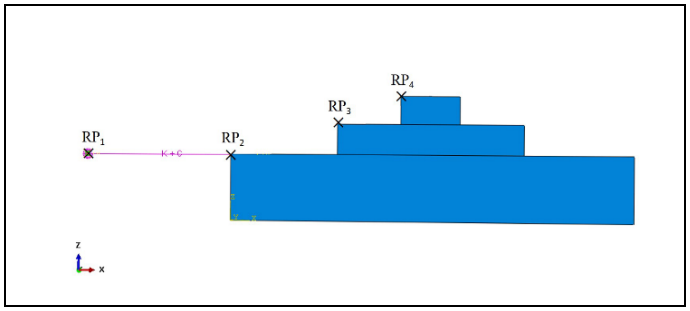

Fig. 6. ABAQUS model of a structure with a two-level stack of SBs.

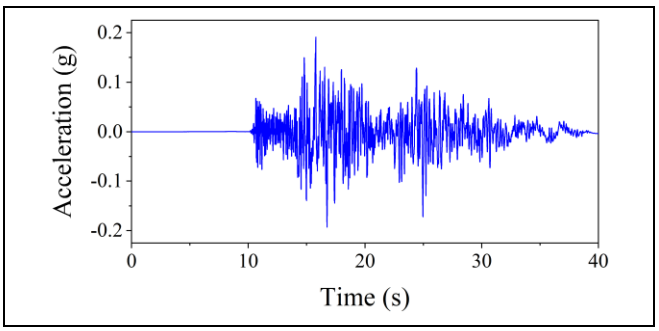

Fig. 7. Acceleration time history used for validation.

Table 1. Details of Earthquake Excitations.

S.No	Event	Year	Station	PGA (g)	Magnitude (M_w)
1	Kern County	1952	Taft Lincoln School	0.18	7.36
2	Loma Prieta	1989	Fremont-Mission San Jose	0.12	6.93
3	Landers	1992	Barstow	0.13	7.28
4	Duzce-Turkey	1999	Lamont 1059	0.15	7.14
5	Chi-Chi	1999	TCU075	0.22	6.2
6	Chi-Chi	1999	CHY028	0.20	6.2
7	Chi-Chi	1999	CHY046	0.12	6.2
8	San Simeon	2003	San Luis Obispo	0.16	6.52
9	Parkfield	1966	Cholame-Shandon Array #12	0.06	6.19
10	Iwate	2008	Semine Kurihara city	0.16	6.9
11	Parkfield	1966	Temblor pre-1969	0.35	6.19

The motion of the rigid bodies is defined by reference nodes assigned to them. A rigid body reference node has both translational and rotational degrees of freedom. Reference node (RP_1) is created to simulate the ground point such that one end of the spring is attached to it, and all degrees of freedom of RP_1 restrained to simulate a fixed point. The other end of the spring element is attached to the primary structure to simulate the SDOF oscillator. Masses of the structure (m_p) and rigid blocks (m_{b1}, m_{b2}) are assigned to the reference nodes as inertia. In this particular study, RP_2, RP_3, and RP_4 are the reference nodes assigned to the primary structure and the rigid sliding blocks, respectively.

The Coulomb friction model is used to capture the friction and sliding at the contact surface. It is a common friction model used to describe the interaction of contact surfaces. The model characterizes the frictional behaviour between the surfaces using a coefficient of friction, μ. To capture the sliding of the blocks under base excitation, the contact interface that exists between the blocks and the SDOF oscillator is modelled via an interaction module in ABAQUS. This is defined by two surfaces designated as master and slave surfaces. Generally, if a smaller surface contacts a larger surface, it is best to choose the smaller surface as the slave surface [25]. The contact interaction between these bodies is generated by the Surface-to-Surface contact (Explicit) method. Explicit method is chosen over the implicit method because the explicit platform will not encounter convergence problems [26]. The normal interaction of the contact is formulated as hard contact, and the tangential interaction is modelled as penalty formulation. The Penalty contact algorithm is used for mechanical constraint formulation [25]. The finite-sliding formulation, which is the most common and allows for sliding of the surfaces in contact, is adopted since small sliding formulation cannot be used for contact pairs using the penalty contact algorithm.

A horizontal acceleration based on earthquake data is applied to the ground point to simulate an excitation at the base of the SDOF oscillator. The structure with a stack of SBs is subjected to a medium hazard spectrum compatible Duzce-Turkey (1999) earthquake recorded at Lamont #1059 station. The acceleration time history of the earthquake used in this validation is shown in Fig. 7.

Figure 8 shows the calculated displacement response for selected values of the mass ratios, coefficients of friction, and period of the structure. It can be observed that SB_1 and the structure behave as one since relative sliding displacement between them is zero. The relative sliding displacement of SB_2 w.r.t SB_1 is more in short period structures since the absolute acceleration of the structure is higher. This conclusion is also observed by the authors in the studies [1], [12]. It is also observed that displacement estimates obtained from the numerical model are identical to those from the FE model.

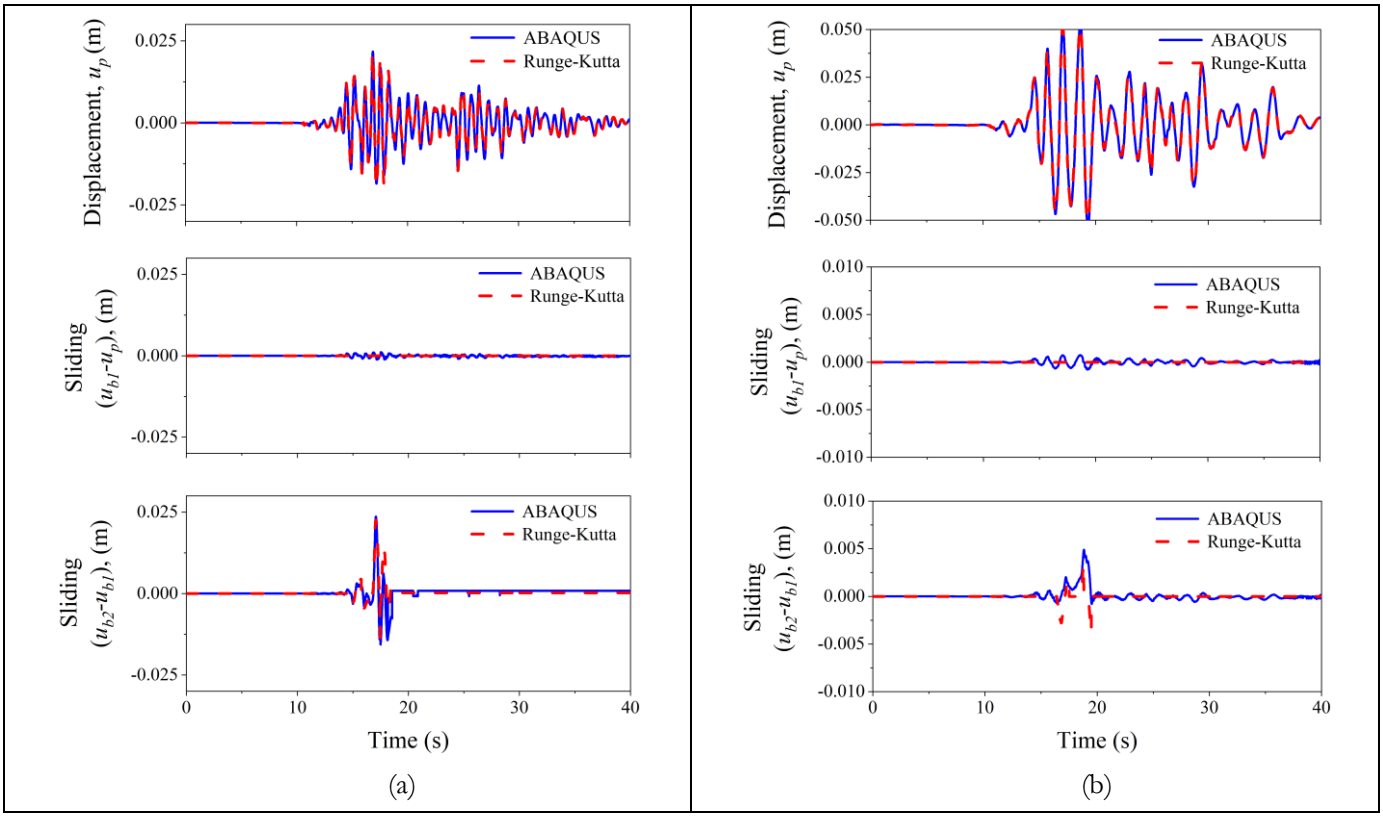

Fig. 8. Comparison of response from Runge-Kutta method and FE model for $\alpha_1 = \alpha_2 = 0.5$, $\mu_1 = 0.3$, $\mu_2 = 0.1$, and: (a) $T_p = 0.5$ s; (b) $T_p = 1$ s.

6. Displacement Response

Previous studies [1], [12]–[14] have focused on the effect of a single sliding rigid block on the dynamic response of its supporting structure. This section investigates the effect of a stack of live load objects on the dynamic response of the structure in comparison to the response of the structure with a single sliding rigid block. Spectra compatible earthquake excitation #11 from Table 1 is applied to the base of the PS with SBs.

A typical structure of the natural period 0.5s is chosen. A mass ratio of 0.5 is used for both α_1 and α_2. Coefficients of friction (μ_1 and μ_2) are 0.3 and 0.1, respectively are chosen to capture the difference in sliding behaviour. For the case where the stack is taken as a single mass, the frictional coefficient between the structure and the sliding mass is kept the same. The displacement response time histories are shown in Fig. 9 for a given earthquake duration (time (t)). Since the maximum displacement of the structure is of great concern for the design of the structures, it is tabulated, as shown in Table 2, for both the seismic hazard levels. It should be noted from Fig. 9 and Table. 2 that there is considerable dissipation of energy due to sliding within the stack for both seismic zones.

6.1. Displacement Response Ratio (*DRR*)

The displacement response of the structure with a stack of SBs is different from that of a structure with a single sliding rigid block, as seen in the previous section. Hence, a parametric study was performed with the following variables: (a) the fundamental period of the structure T_p; (b) the blocks-to-structure mass ratios α_1 and α_2; (c) the coefficients of friction at the interface of SBs; SB_1 and PS i.e., μ_1 and μ_2 respectively. Different analysis runs were analysed as a result of different variable permutations for each seismic damage risk zone. Each run involves the calculation of the mean of the maximum displacement response of the system for scaled eleven ground motions. A set of parameters is defined to quantify the effect of a stack of SBs on the response of the primary structure and are called Displacement Response Ratios (*DRR*).

$$DRR_1 = \frac{(u_p)_{stack}}{(u_p)_{rigid}} \tag{7}$$

$$DRR_2 = \frac{(u_p)_{single}}{(u_p)_{rigid}} \tag{8}$$

where $(u_p)_{stack}$ is the displacement of a structure supporting a stack of SBs and $(u_p)_{single}$ is the displacement of the same structure but supporting a single sliding block of the same as whole stack.

$(u_p)_{rigid}$ is the displacement of the structure supporting an equivalent rigidly attached block (with the same mass as the stack). DRR_1 or DRR_2 approaching one indicates minimal slippage.

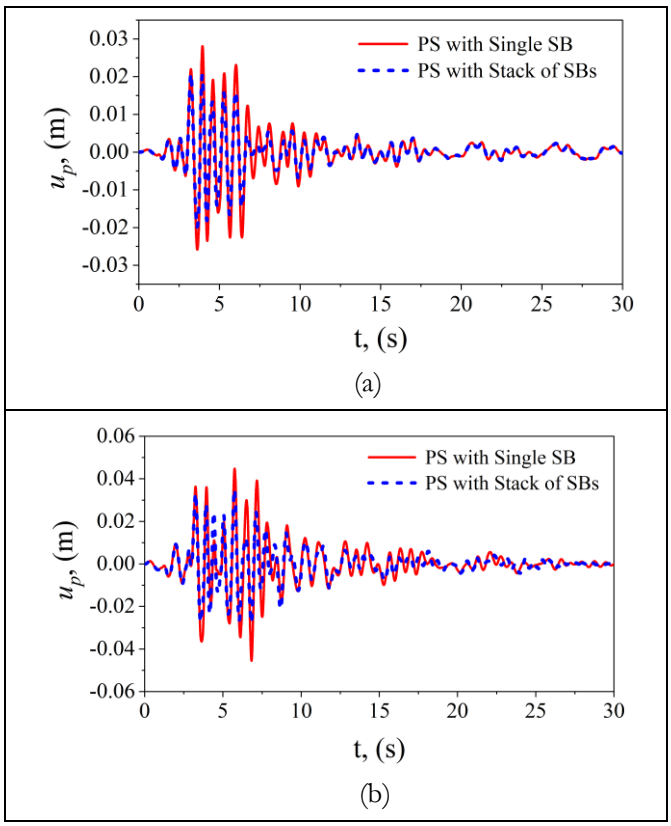

Fig. 9. Displacement response of the PS (a) Zone III (b) Zone V.

Table 2. Maximum displacement of the PS.

Maximum displacement of the PS, u_p (m)			
Seismic Zone	PS with a Single SB	PS with a Stack of SBs	% reduction
III	0.028	0.021	25
V	0.046	0.035	23.91

If the ratio of DRR_1 to DRR_2 approaches one, it indicates that slippage within the stack is not significant.

The values of *DRR* increase significantly with the period of the structure and the coefficient of friction, as shown in Fig. 10 for medium damage risk zone, especially for larger values of the mass ratio. A practical implication that can be drawn from Fig. 10 is that if $\mu_2 \leq \mu_1$, input energy is dissipated by the relative movement between blocks since $DRR_1 < DRR_2$. For $\mu_2 > \mu_1$, no energy dissipation is observed within the stack ($DRR_1 = DRR_2$). This is due to the fact that when the lower block (SB_1) in a stack is sliding, and upper block (SB_2) is at rest with respect to SB_1, then the resistant force acting on SB_2 is given as $m_{b2}(\ddot{u}_{b1} + \ddot{u}_g) = f_1$. The resistant force f_1 can be obtained from the Eq. (3) and is as follows:

$$f_1 = -m_{b2}\mu_{k1}gsign(\dot{u}_{b1} - \dot{u}_p) \quad (9)$$

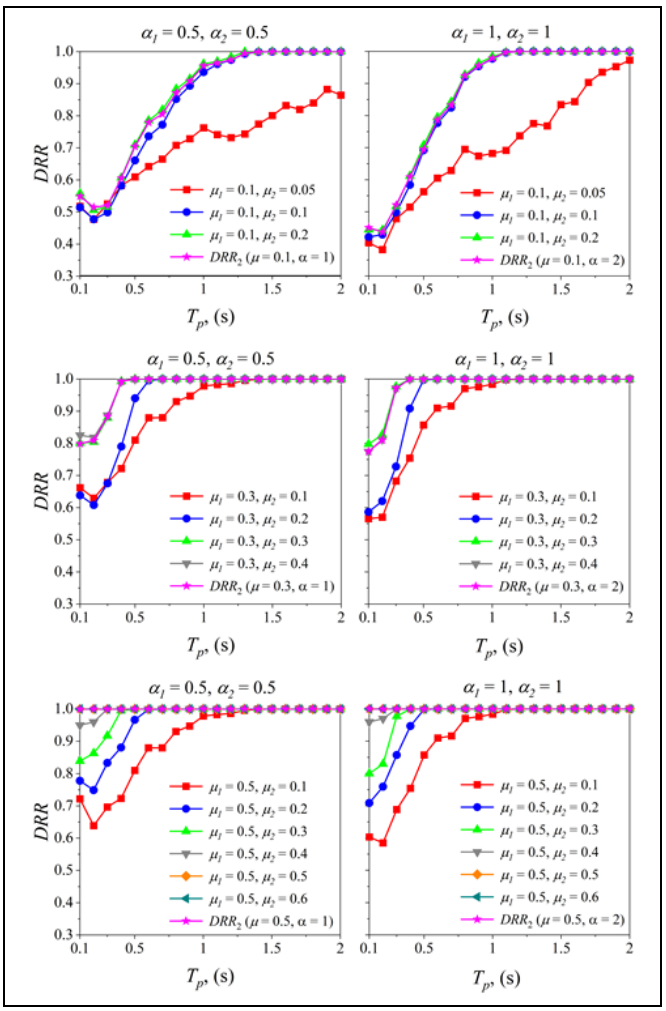

Fig. 10. Displacement Response Ratio (DRR) for primary structure under medium seismic damage risk zone (Zone III).

The rigid block on the top m_{b2}, starts sliding only when f_1 exceeds the limiting static frictional force between m_{b1} and m_{b2} i.e.,$m_{b2}\mu_{s2}g = f_2$. Since $\mu_{k1} < \mu_{k2}$, f_1 will never reach the value of the limiting frictional force f_2 and hence m_{b2} will not slide when the lower block (SB_1) slides with respect to the structure. Hence, in this case, the energy dissipation due to friction within the stack is negligible and the two rigid blocks in the stack behave as a single block ($m_{b1} + m_{b2}$).

From Fig. 11, it is observed that DRR increases significantly with an increase in the natural time period of the structure and the coefficients of friction as expected. The same trend is seen for DRR in the highest damage risk zone also. Energy dissipation due to friction between the stack of blocks is negligible when $\mu_2 > \mu_1$ similar to medium damage zone. Hence from Figs. 10 and 11, it can be concluded that regardless of seismic damage risk zone, mass ratios and friction coefficients if $\mu_2 > \mu_1$, stack of rigid blocks can be considered as a single sliding rigid block.

Due to the sliding of the stack of blocks and within the stack, only a portion of the total mass of the stack participates in the primary structural inertia [1], [12], [13].

This affects the modal characteristics of the primary structure. In this study, an equivalent time period for the structure is evaluated for understanding this behavior.

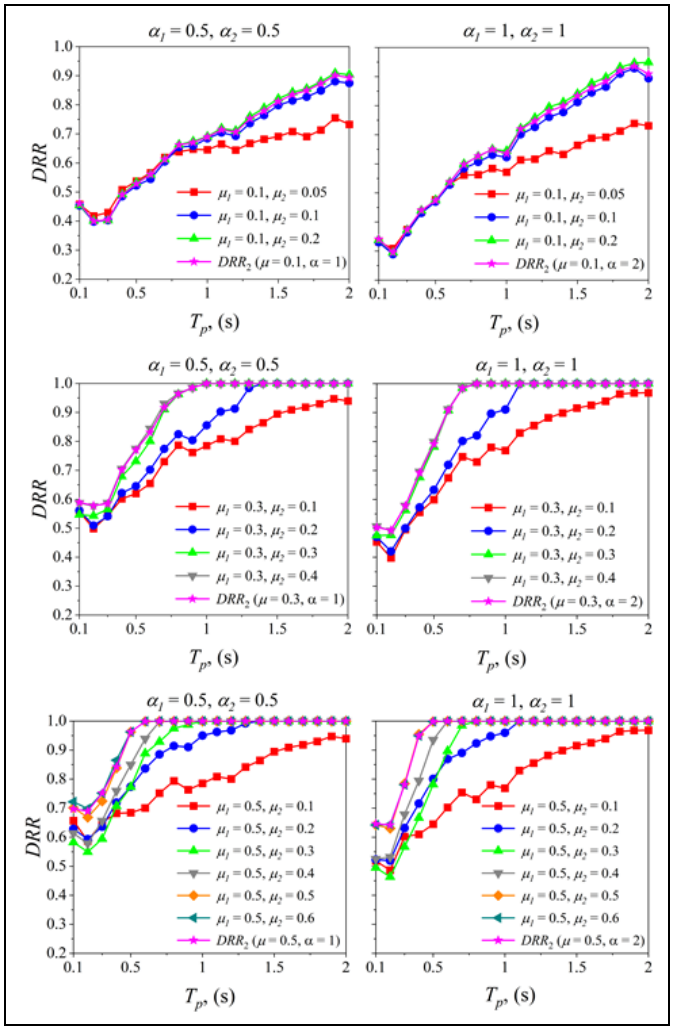

Fig. 11. Displacement Response Ratio (DRR) for primary structure under highest seismic damage risk zone (Zone V).

7. Modified Structural Period

This section explains a methodology to determine an equivalent time period for the structure termed as a modified structural period (T_{new}). When the bodies are rigidly attached to the structure, the structural period of the structure is given as:

$$T_{rigid} = 2\pi\sqrt{\frac{m_p + m_{b1} + m_{b2}}{k}} \tag{10}$$

Replacing m_{b1} and m_{b2} with $\alpha_1 m_p$ and $\alpha_2 m_p$ in the above expression, then it becomes:

$$T_{rigid} = 2\pi\sqrt{\frac{m_p + \alpha_1 m_p + \alpha_2 m_p}{k}} \tag{11}$$

$$T_{rigid} = 2\pi\sqrt{\frac{m_p}{k}}\sqrt{(1 + \alpha_1 + \alpha_2)} \tag{12}$$

Replacing $2\pi\sqrt{\frac{m_p}{k}}$ in the above expression with T_p, Eq. (12) reduces to

$$T_{rigid} = T_p\sqrt{(1 + \alpha_1 + \alpha_2)} \tag{13}$$

Equation (13) gives the structural period of the PS when the SBs are rigidly attached to it. The following section explains a procedure to determine the structural period of the primary structure when the SBs are sliding. $T_{new} = T_{rigid}$, when SBs are rigidly attached to the PS.

7.1. Methodology for determination of T_{new}

The procedure to determine the T_{new} is outlined below for a given set of values of T_p , μ_1, μ_2, α_1 and α_2.

1. Calculate the absolute maximum accelerations of the structure (m_p) and lower body in the stack (m_{b1}) for the eleven scaled ground motions (Section 4) for a given seismic hazard level. If accelerations of m_p and m_{b1} are less than $\mu_1 g$ and $\mu_2 g$ respectively, then the blocks will not slide and therefore $T_{new} = T_{rigid}$. Otherwise, the sliding will be seen within the stack and below the stack.
2. Calculate the mean of the 5%-damping displacement spectrum for the set of scaled ground motions for various structural periods(T_p).
3. Calculate the mean of the maximum displacement of the PS with a stack of sliding SBs for a given set of scaled eleven ground motions using the numerical procedure shown in Fig. 2.
4. Determine the structural period from the 5%-damping mean displacement spectrum (obtained in Step (2)) for the calculated mean displacement (obtained in Step (3)) by linear interpolation.

The process is illustrated in Fig. 12. Structural period of the PS with stack of SBs is evaluated under scaled eleven ground motions for T_p = 1 s, $\alpha_1 = \alpha_2 = 0.5$, $\mu_1 = 0.2$ and $\mu_2 = 0.1$ in this case. The mean displacement of the PS is found out to be 5.49 cm. The corresponding structural period of the structure using the methodology is 1.38 s.

7.2. Validation of the proposed methodology

The proposed methodology for the calculation of the structural period of the PS needs to be validated before

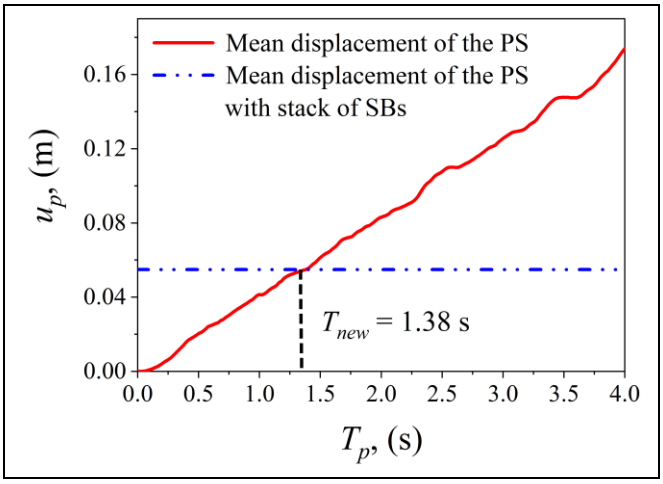

Fig. 12. Determination of the T_{new} of a PS with a stack of sliding SBs.

proceeding to conduct parametric studies. For such validation, the algorithm proposed for the calculation of the portion of the mass of SB in the primary structure inertia given in the study [12] is utilized in the present study. The target spectrum for operating level (OLE) seismic hazard utilized in the study [1] is taken from [27], and the ground motions scenario mentioned in the study [1] is used for the validation. Fig. 13 shows the mean spectrum of the scaled ground motions using the scaling procedure given in the ASCE 7-10 and the target spectrum for the OLE seismic hazard. Since the study [12] is for a structure with a single live load object, SB_2 is considered to be rigidly attached to the SB_1 Thus, Eq. (13) becomes:

$$T_{rigid} = T_p\sqrt{(1+\alpha)} \tag{14}$$

The structural period of the PS due to the live load object interaction is given as [12]:

$$T_\lambda = T_p\sqrt{(1+\alpha\lambda)} \tag{15}$$

where, λ is the portion of live load object participates as inertia in the primary structure [12].

From the example calculation of the live load as inertia for OLE seismic hazard in the study [12], the structural period of the PS for given input parameters is 0.86s. The same input parameters are used, and the structural period is calculated by the methodology proposed in section 7.1 of the present study, as shown in Fig. 14 by considering the OLE level mean spectrum as a design spectrum.

T_{new}= 0.858 s obtained from Fig. 14 by using the methodology in section 7.1. This result is in agreement with the structural period is obtained through the portion of the live load (λ) in the study [12]. Fig. 15 shows the comparison of the structural period of PS with a stack of SBs (T_{new}) obtained by the methodology described in section 7.1 with an existing study. Input parameters μ_1 = 0.1, α_1 = 0.4, α_2 = 0.35 are chosen. The SB_2 is assumed to be rigidly fixed to the SB_1 (neglect energy dissipation due to friction between SB_1 and SB_2), i.e., mass ratio,$\alpha = 0.75$. It can be observed that T_{new} obtained by the proposed methodology agrees with the previous study [12].

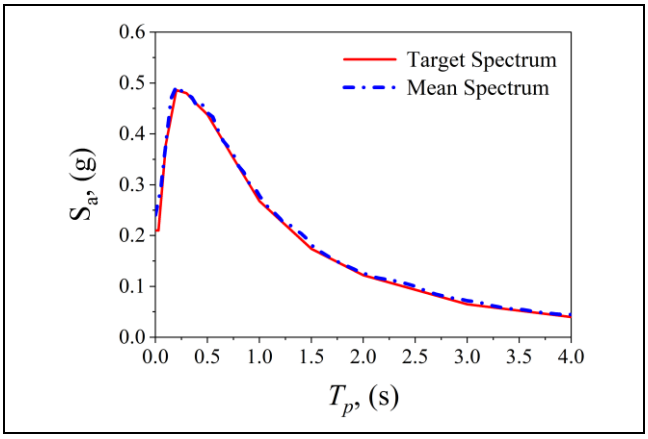

Fig. 13. Target and Mean acceleration spectra for OLE level for 5% damping.

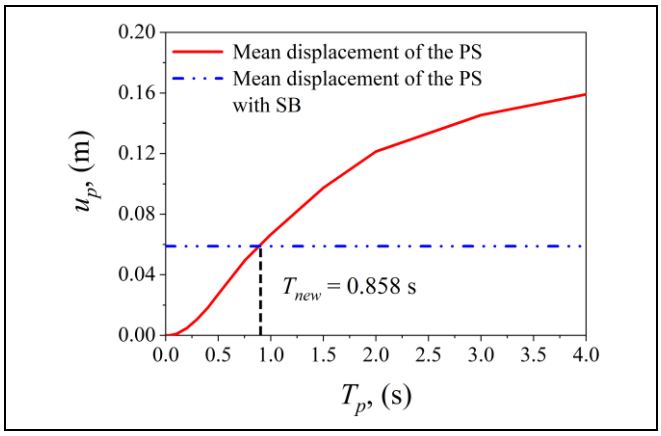

Fig. 14. Determination of the structural period of a PS with SB for OLE level.

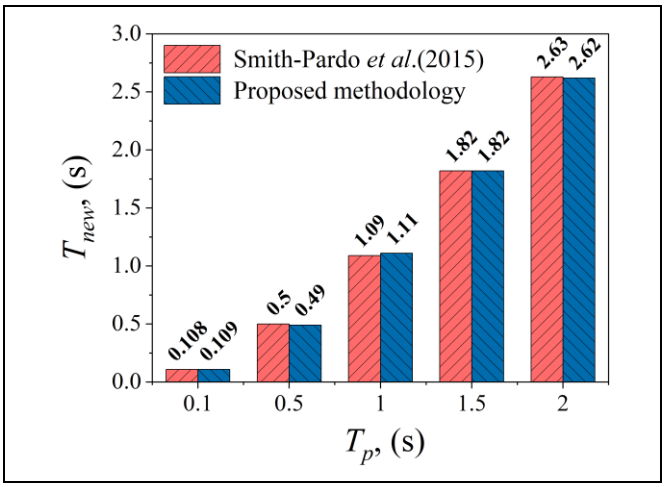

Fig. 15. Validation of the proposed methodology for T_{new} with an existing study.

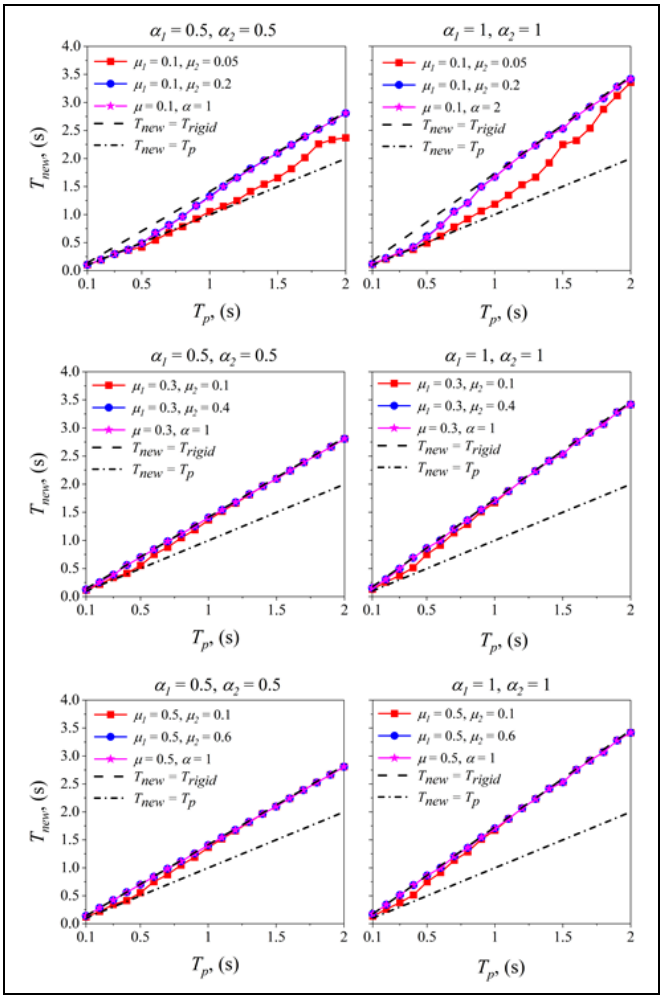

Fig. 16. T_{new} against T_p for medium seismic hazard level (Zone III).

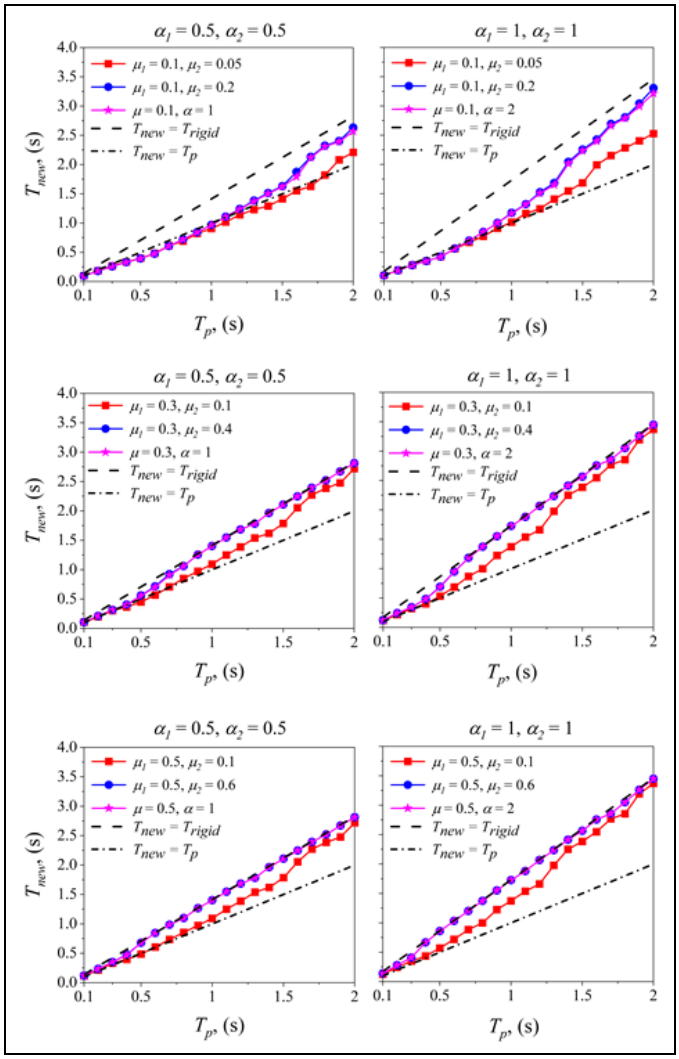

Fig. 17. T_{new} against T_p for highest seismic hazard level (Zone V).

7.3. Variation of T_{new} with T_p

A parametric study was performed with: (a) the fundamental period of the structure T_p (from 0.1 s to 2 s, increments of 0.1 s); (b) the blocks-to-structure mass ratios α_1 and α_2 (0.1, 0.5, 1.0); (c) the coefficient of friction at the interface of SBs; SB_1 and PS. $\mu_1 = 0.05$, 0.1 to 0.6 (with increments of 0.1) and $\mu_2 = 0.05$, 0.1 to 0.7 (with increments of 0.1). A total of 6300 analysis runs are analyzed as a result of different variable permutations for each seismic damage risk zone. Each run involves the calculation of the modified structural period (T_{new}).

Figure 16 shows a subset of results from the parametric study for a given mass ratio and coefficients of friction. It is observed that T_{new} increases with the coefficients of friction and structural period. The increase in T_{new} is significant at higher mass ratios. The structural period of the PS with a stack of SBs is equal to the structural period of the PS with a single sliding rigid block when $\mu_2 > \mu_1$.

The modified structural period (T_{new}) increases with the original structural period and coefficients of friction, especially for larger values of mass ratios, as shown in Figs. 16 and 17 under either seismic hazard levels.

Energy dissipation associated with the relative movement between blocks can be neglected when $\mu_2 > \mu_1$. It can be observed that energy dissipation due to friction between the blocks is more in the highest seismic hazard level compared to the medium seismic hazard level.

8. Proposed Design Equation for T_{new}

In order to design a structure with a given stack of sliding bodies by response spectrum method, an equation for T_{new} needs to be developed. For some of the cases, T_{new} can be obtained from Figs. 16 and 17. In other cases, a design equation will be developed through a parametric study by considering a large number of discrete points correspond to various variables. This study comprised of the variables and ranges of values, as mentioned in section 7.3. Non-Linear Regression (NLR) analyses yield the following design equations to calculate T_{new} for each seismic damage risk zone:

For Medium seismic hazard zone:

$$T_{new} = \Big((-4.284 * T_p) - (0.173s * \mu_1) + (0.015s * \mu_2) - (4.365s * \alpha_1) - (4.567s * \alpha_2)\Big) + 2.022s * e^{\left(\left(\frac{0.053}{s} * T_p\right) + (0.003 * \mu_1) + (0.002 * \mu_2) + (0.044 * \alpha_1) + (0.045 * \alpha_2) + 3.873\right)} - 97.3s \quad (16)$$

For Highest seismic hazard zone:

$$T_{new} = \Big((-5.464 * T_p) - (2.268s * \mu_1) - (4.451s * \mu_2) - (5.064s * \alpha_1) - (4.693s * \alpha_2)\Big) + 2.197s * e^{\left(\left(\frac{0.052}{s} * T_p\right) + (0.02 * \mu_1) + (0.038 * \mu_2) + (0.041 * \alpha_1) + (0.038 * \alpha_2) + 3.97\right)} - 116.3s \quad (17)$$

The prediction capability of the regression models for both the seismic zones are evaluated by defining the various statistical performance functions like Co-efficient of Determination (R^2), Correlation Coefficient (R), Root Mean Square Error (RMSE), Mean Square Error (MSE) and Mean Absolute Error (MAE). The performance of the models is summarized in Table. 3.

Table 3. Performance of the regression models.

Seismic Zone	R^2	R	RMSE	MSE	MAE
III	0.985	0.992	0.094	0.009	0.082
V	0.969	0.985	0.1	0.01	0.09

The R-value of the model should be as high as possible since it gives the relative correlation and goodness of the fit between the measured and predicted values. RMSE, MSE, and MAE are errors, and they should be as low as possible [28]. A strong correlation exists between the measured and predicted values if R > 0.8 [29]. Therefore, from Table. 3, it can be observed that the strong correlation exists between the measured and predicted values with minimum errors.

9. Numerical Example

A numerical example has been provided to explain the process of structural period calculation using the developed equations.

Problem Statement : Find the modified time period (T_{new}) for a structure with a natural time period of 0.7 s. and coefficients of friction μ_1 = 0.3 and μ_2 = 0.1 with mass ratios of SBs $\alpha_1 = \alpha_2 = 1$ for Zone III and Zone V seismic hazard levels.

Solution:

Given data: T_p = 0.7 sec; μ_1 = 0.3; μ_2 = 0.1; α_1 = 1; α_2 = 1

The values of modified structural period of the PS (T_{new}) obtained from Eq. (16) and Eq. (17) for Seismic zones III and V are **1.14 sec** and **0.92 sec** respectively. The design spectral accelerations (S_a) of the PS without SBs in Zones III and V for a given T_p can be obtained from Fig. 5 and are 0.22g and 0.52g, respectively. Due to the interaction of the stack of SBs, the structural period increases to 1.14 sec and 0.92 sec in Zones III and V, respectively. Thus the design spectral accelerations of the PS in medium and highest seismic hazard levels are 0.14g and 0.31g, respectively. These parameters should be used in the seismic analysis and design of the PS.

10. Summary and Conclusions

The objective of this paper is to study the effect of a single stack of live load objects on the seismic behavior of a structure. A numerical model that describes the response of the primary structure supporting a stack of rigid blocks with a possibility to slide was developed. The governing equations of motion were derived for primary structure and secondary bodies by considering Coulomb's friction model and were solved using the 4th order Runge-Kutta method. In this paper, the results are limited to a two-body stack for simplicity. The methodology remains the same for larger stacks.

Spectrum compatible ground motions were applied to the structure. An extensive parametric study has been conducted to verify the effect of various parameters such as structural period, mass ratios, and coefficients of friction on the seismic response of the structure. A methodology was developed to determine the modified structural period of the structure due to the interaction of a stack of sliding rigid blocks. From this study, it can be concluded that:

- The seismic behaviour of the primary structure is greatly affected by a stack of live load objects under real earthquake ground motions.
- Displacement estimates of the primary structure are found out to be conservative by neglecting energy dissipation associated with the relative movement of rigid blocks in the stack. Energy dissipation within the stack depends upon the coefficient of friction, mass ratios, and level of excitation.
- Energy dissipation associated with the relative movement between rigid blocks is more in the highest damage risk zone than the medium damage zone for a given problem.
- Under both medium and highest damage risk zones, the displacement response of the structure increases significantly with an increase in the structural period, mass ratios, and coefficients of friction.
- Regardless of the seismic damage risk zone, mass ratios, and coefficient of friction values, if $\mu_2 > \mu_1$, the energy dissipation within the stack can be neglected.

- A novel methodology was developed to determine the modified structural period (T_{new}) of the primary structure due to the interaction of a stack of sliding rigid blocks.
- T_{new} increases significantly with the original structural period and coefficients of friction, especially for larger mass ratios.
- Design equations were developed to determine the T_{new} as a function of structural period, coefficients of friction, and mass ratios for a given seismic hazard level by Non-Linear Regression (NLR).
- Since, T_{new} generally is less than T_{rigid} and more than T_p, the calculation of T_{new} is essential for design of such structures.

The proposed methodology in the present study is limited to an idealized linear SDOF structure. The numerical model developed in this study captures non-linearity due to the sliding of the rigid blocks. The coupled non-linearity due to the sliding of the blocks and the yielding of the structure will be incorporated in the numerical model in future studies. The more generalized conclusions can be drawn by looking at the actual complex MDOF structures behavior with stacked sliding loads at various story levels through non-linear incremental dynamic analysis (IDA). The present study can be a preliminary study for future studies in this aspect, and the proposed design equations can be modified for the MDOF structures whose seismic behavior is affected by the higher modes.

References

[1] J. P. Smith-Pardo, J. C. Reyes, O. A. Ardila-Giraldo, L. Ardila-Bothia, and J. N. Villamizar-Gonzalez, "Dynamic effect of sliding rigid blocks on the seismic response of structures," in *Second European Conference on Earthquake Engineering and Seismology, Istanbul*, 2014, pp. 25–29.

[2] K. Matsui, M. Iura, T. Sasaki, and I. Kosaka, "Periodic response of a rigid block resting on a footing subjected to harmonic excitation," *Earthq. Eng. Struct. Dyn.*, vol. 20, no. 7, pp. 683–697, 1991, doi: 10.1002/eqe.4290200707.

[3] A. Saraswat, G. R. Reddy, A. K. Ghosh, and S. Ghosh, "Effects of base excitation frequency on the stability of a freestanding rigid block," *Acta Mech.*, vol. 227, no. 3, pp. 795–812, 2016, doi: 10.1007/s00707-015-1484-2.

[4] B. Choi and C. C. D. Tung, "Estimating sliding displacement of an unanchored body subjected to earthquake excitation," *Earthq. Spectra*, vol. 18, no. 4, pp. 601–613, 2002, doi: 10.1193/1.1516750.

[5] R. F. Shie, K. Ting, J. S. Yu, and C. T. Liu, "The sliding and overturning analysis of a free-standing cask under earthquake," *Solid State Phenom.*, vol. 120, pp. 207–212, 2007, doi: 10.4028/www.scientific.net/SSP.120.207.

[6] Q. Zhou and W. Yan, "Sliding response of free-standing cultural relics under earthquakes by simulation," *Adv. Mater. Res.*, vol. 163–167, pp. 2142–2146, 2010, doi: 10.4028/www.scientific.net/AMR.163-167.2142.

[7] K. Furuta, T. Ito, and A. Shintani, "Rocking and sliding motions of a freely standing structure coupled with inner structure," in *ASME 2008 Pressure Vessels and Piping Conference*, 2008, pp. 97–103.

[8] C. Younis and I. Tadjbakhsh, "Response of sliding rigid structure to base excitation," *J. Eng. Mech.*, vol. 110, no. 3, pp. 417–432, 1984, doi: 10.1061/(ASCE)0733-9399(1984)110:3(417).

[9] T. Okada and K. Takanashi, "The resonance responses of steel structure with sliding floor loads," in *Proc. 10th World Conf. on Earthquake Engineering, Madrid*, 1992, vol. 3, pp. 4419–4422.

[10] A. R. Chandrasekaran and S. S. Saini, "Live load effect on dynamic response of structures," *J. Struct. Div.*, 1969.

[11] O. A. Ardila-Giraldo, J. C. Reyes, and J. P. Smith-Pardo, "Contact interface modeling in the dynamic response of rigid blocks subjected to base excitation," *ECCOMAS Themat. Conf. - COMPDYN 2013 4th Int. Conf. Comput. Methods Struct. Dyn. Earthq. Eng. Proc. - An IACM Spec. Interes. Conf.*, no. June, pp. 3060–3071, 2013.

[12] J. P. Smith-Pardo, J. C. Reyes, L. Ardila-Bothia, J. N. Villamizar-Gonzalez, and O. A. Ardila-Giraldo, "Effect of live load on the seismic design of single-story storage structures under unidirectional horizontal ground motions," *Eng. Struct.*, vol. 93, pp. 50–60, 2015, doi: 10.1016/j.engstruct.2015.03.020.

[13] J. C. Reyes, L. Ardila-Bothia, J. P. Smith-Pardo, J. N. Villamizar-Gonzalez, and O. A. Ardila-Giraldo, "Evaluation of the effect of containers on the seismic response of pile-supported storage structures," *Eng. Struct.*, vol. 122, pp. 267–278, 2016, doi: 10.1016/j.engstruct.2016.04.051.

[14] J. C. Reyes, E. Marcillo-Delgado, J. P. Smith-Pardo, and O. A. Ardila-Giraldo, "Assessment of the effective seismic mass for low-rise framed shear buildings supporting nearly permanent live loads," *J. Struct. Eng.*, vol. 144, no. 8, p. 04018098, 2018, doi: 10.1061/(ASCE)ST.1943-541X.0002121.

[15] M. Bayat, H. R. Ahmadi, M. Kia, and M. Cao, "Probabilistic seismic demand of isolated straight concrete girder highway bridges using fragility functions," *Adv. Concr. Constr.*, vol. 7, no. 3, pp. 183–189, 2019.

[16] H. R. Ahmad, N. Namdari, M. Cao, and M. Bayat, "Seismic investigation of pushover methods for concrete piers of curved bridges in plan," *Comput. Concr.*, vol. 23, no. 1, pp. 1–10, 2019.

[17] H. R. Ahmadi, N. Mahdavi, and M. Bayat, "Applying adaptive pushover analysis to estimate incremental dynamic analysis curve," *J. Earthq.*

Tsunami, 2020.
[18] A. Ketsap, C. Hansapinyo, N. Kronprasert, and S. Limkatanyu, "Uncertainty and fuzzy decisions in earthquake risk evaluation of buildings," *Eng. J.*, vol. 23, no. 5, pp. 89–105, 2019.
[19] S. Panyamul, P. Panyakapo, and A. Ruangrassamee, "Seismic Shear Strengthening of Reinforced Concrete Short Columns Using Ferrocement with Expanded Metal," *Eng. J.*, vol. 23, no. 6, pp. 175–189, 2019.
[20] P. Center, "PEER ground motion database," Pacific Earthq. Eng. Res. Center, Univ. California, Berkeley, CA, 2013. [Online]. Available: http//ngawest2. berkeley.edu
[21] *Minimum Design Loads and Associated Criteria for Buildings and Other Structures*, ASCE/SEI 7-16, 2016.
[22] *Criteria for Earthquake Resistant Design of Structures*, IS 1893: 2016,
[23] K. Khy, C. Chintanapakdee, and A. C. Wijeyewickrema, "Application of conditional mean spectrum in nonlinear response history analysis of tall buildings on soft soil," *Eng. J.*, vol. 23, no. 1, pp. 135–150, 2019, doi: 10.4186/ej.2019.23.1.135.
[24] L. Alatik and N. Abrahamson, "An improved method for nonstationary spectral matching," *Earthq. Spectra*, vol. 26, no. 3, pp. 601–617, 2010, doi: 10.1193/1.3459159.
[25] D. S. Dassault Systèmes, "Abaqus analysis user's guide," Technical Report Abaqus 6.14 Documentation, Simulia Corp, 2016.
[26] M. Zhang, R. Jiang, and H. Nie, "A numerical study on the friction and wear predictions of finger lock chuck in landing gear," in *Proc. Inst. Mech. Eng. Part G J. Aerosp. Eng.*, 2017, vol. 231, no. 1, pp. 109–123, doi: 10.1177/0954410016650710.
[27] E. Mechanics, "Port-wide ground motion study port of Long Beach," Final Rep., 2006.
[28] S. Debnath and P. Sultana, "Prediction of settlement of shallow foundation on cohesionless soil using artificial neural network," in *7th Indian Young Geotechnical Engineers Conference– 7IYGEC 2019*, NIT Silchar, Assam, India, 15-16 March 2019.
[29] G. N. Smith, *Probability and Statistics in Civil Engineering*. Collins, 1986.

Surya Prakash Challagulla, photograph and biography not available at the time of publication.

Chandu Parimi, photograph and biography not available at the time of publication.

P. K. Thiruvikraman, photograph and biography not available at the time of publication.